

Model and Software Package for Studying and Optimizing Generation Characteristics of Semiconductor Superlattices

V. V. Makarov, A. O. Selskii, V. A. Maksimenko, A. A. Koronovskii,
O. I. Moskalenko, and A. E. Hramov*

Gagarin State Technical University, Saratov, Russia

Chernyshevskii State Technical University, Saratov, Russia

*e-mail: hramovae@gmail.com

Received September 9, 2015

Abstract—A software package for simulating the dynamics of semiconductor superlattices under the influence of an external magnetic field is developed. The analytical and numerical models on which the program package is based are described in detail in the paper. The approbation of the developed package shows that it can be effectively used to study the dynamics of semiconductor superlattices, including the optimization of the generation characteristics of subterahertz and terahertz devices.

DOI: 10.1134/S2070048217030097

1. INTRODUCTION

Mastering the terahertz range of frequencies is a new direction in contemporary radiophysics, electronics, and photonics, which is being actively developed. The urgency and interest in promoting semiconductor electronic devices of the microwave range to areas of higher frequencies are due to the following circumstance (see [1, 2]): currently, the terahertz range (especially between 0.3 THz and 3 THz) is one of the least mastered ranges in electronics and quantum radiophysics. Located outside the operating limits of traditional microwave and optic devices, it belongs to the so-called terahertz gap (see [3]). Nowadays, terahertz technologies are especially important for developing the terahertz-range spectroscopy, wireless high-frequency data-communication devices, systems of radio-wave imaging and security, etc. (see [2, 4–6]).

A semiconductor superlattice, which is a structure consisting of alternating layers of several layers (usually, two layers) of semiconductor materials with different widths of the prohibited zone (see [7–9]), is a promising nanoelectronic semiconductor device able to generate subterahertz and terahertz waves in a wide range of operational temperatures, including room temperature. Applying an electric field to such a periodic nanostructure, we observe the formation of moving charge domains whose frequency factor varies from dozens of THz to hundreds of THz and depends on the physical parameters of the structure and various external parameters, such as the contact parameters and the applied magnetic field (see [10, 11]). This provides a possibility to use superlattices as the domain transport in the generators and amplifiers of the subterahertz and terahertz ranges (see [12, 13]).

Since a semiconductor superlattice is an active nonlinear medium that allows various oscillation modes depending on many control parameters to be implemented in it, it follows that numeric simulations and experimental investigations are needed to study the characteristics of semiconductor superlattices in detail and optimize them. However, it is hard and expensive to grow experimental samples of nanostructures. This explains the interest in the numeric simulation of the dynamics of the spatial charge in a semiconductor superlattice and the prediction of the characteristics of the generation and amplification of signals depending on the physical parameters of the nanostructure (e.g., the minizone width) and external parameters such as the temperature, resistance of the contacts, and the external oscillating system. In practice, it is especially important to simulate the charge transport in the investigated nanostructure under the influence of an external tilted magnetic field (see [14]) because this field is able to deeply affect its behavior, increasing the frequency and power of the generated oscillations (see [15, 16]).

Thus, there is interest in creating a software package aimed at numerically simulating the spatial-temporal dynamics of the charge in a semiconductor superlattice under the influence of an external electric field and a tilted magnetic field. The most universal approach to simulate the charge transportation in a

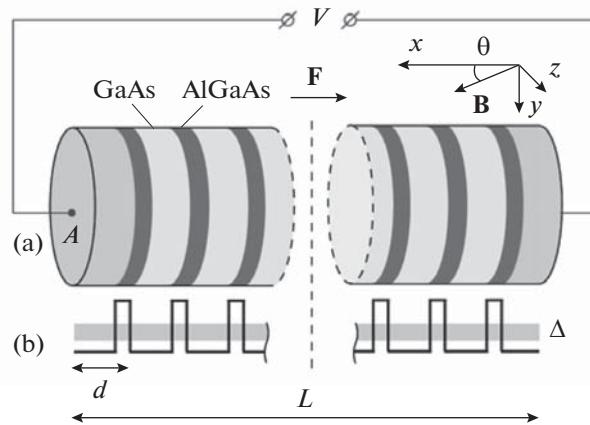


Fig. 1. Layers of semiconductor superlattice (a) and scheme of zone structure (b).

semiconductor superlattice is the so-called semiclassical approach (see [17, 18]) based on the assumption that the tunnel effect between minizones (the Landau–Zener tunnel effect) can be disregarded and, therefore, it suffices to consider the transport of electrons only in the first minizone. Such an approach can be implemented by the self-consistent model consisting of continuity equations and Poisson equations, where the dependence of the drift velocity of the charge carriers is computed by the approach proposed by Esaki and Tsu (see [8, 19, 20]). Such a mathematical model does not require much computational capacity, but it is consistent with the experimental results of the study of superlattices. The software package described in the present paper is based on this mathematical model.

2. MATHEMATICAL MODEL

2.1. Semiconductor superlattices: the investigated model. The investigated model of a semiconductor superlattice is displayed in Fig. 1a. We consider a superlattice with length L and cross-section area A , consisting of alternating layers of two semiconductors with different widths of the prohibited zone (for the specified figure, GaAs and AlGaAs are selected as examples). For such a structure, the electron potential can be described by the periodic one-dimensional model of rectangular wells and barriers called the Kronig–Penney model (see Fig. 1b). In this model, the wave functions of the electrons in the two neighboring wells overlap each other and the system of energy levels of the atoms is transformed to a system of energy minizones (the width of the minizone depends on the width of the barrier) such that the electrons inside the minizones can freely tunnel and move along the direction orthogonal to the layers (see [17]). For simplicity, only the first minizone Δ is displayed at Fig. 1b; the electron transport is considered within it. We restrict our consideration to the case where the minizone width exceeds 10 meV, which implies that the electron transport in the nanostructure is provided mainly by the minizone tunnel effect; such structures are called tightly bound superlattices (see [18]). The coordinate axes illustrate the orientation of the magnetic induction vector \mathbf{B} lying in the plane x – z and inclined at angle θ with respect to axis x . The direction of vector \mathbf{F} of the electric field strength is opposite to the direction of the coordinate axis x . A constant voltage V is applied to the contacts of the superlattice. Once the voltage V exceeds the threshold value (coinciding with the beginning of the Bloch oscillations), domains of a high concentration of the charge arise in the nanostructure and move from the emitter of the superlattice to its collector.

2.2. Charge transport in semiconductor superlattices: mathematical model. To simulate the charge dynamics in a nanostructure, we use the self-consistent system of the continuity equations and the Poisson equation. Denote the electron concentration by $n(x, t)$, where x is the longitudinal coordinate in the superlattice and t is the time, and denote the value of the electric field strength by $F(x, t)$. Then the evolution of the charge density is described by the continuity equation

$$e \frac{\partial n}{\partial t} = - \frac{\partial J}{\partial x}, \quad (1)$$

where $J(x, t)$ is the density of the current elapsing through the cross section of the superlattice, and $e > 0$ is the electron charge. In the drift approximation, the current density $J(x, t)$ can be found by the relation

$$J = en(x, t)v_d(F(x, t)), \quad (2)$$

where $v_d(x, t)$ describes the drift electron velocity for the value $F(x, t)$ of the electric field strength (see [19]). Note that the external tilted magnetic field B is not explicitly included in the equations describing the dynamics of the charge domains, but it substantially affects the character of the dependence of the drift velocity on the electric field strength $v_d(F)$. Hence, it also affects the dynamical modes of the semiconductor superlattice (see [18–20]). If a magnetic field exists, then the dependence of the drift velocity on the electric field strength cannot be found analytically [21]. For the case where $B = 0$ tesla, the dependence of the drift velocity $v_d(F)$ can be analytically represented as follows (see [22]):

$$v_d = v_0 \frac{\tau \omega_B}{1 + \tau^2 \omega_B^2}, \tag{3}$$

where $\omega_B = eFd/\hbar$ is the frequency of the Bloch oscillations.

The Poisson equation

$$\frac{\partial F}{\partial x} = \frac{e}{\epsilon_0 \epsilon_r} (n_m - n_D), \tag{4}$$

where n_D describes the equilibrium concentration of electrons determined by the alloying level, while ϵ_0 and ϵ_r denote the electric constant and the relative dielectric constant of the material respectively, is solved self-consistently and simultaneously with Eq. (1). To simulate processes in the superlattice properly, one has to take into account the processes taking place at the boundaries of the semiconductor nanostructure. This means that the influence of the contacts has to be taken into account. If ohmic contacts on the emitter and collector of the superlattice are assumed, then the density J_0 of the current through the emitter is determined by the conductivity $J(0, t) = \sigma F(0, t)$ of the contact σ , while the electric field strength $F(0, t)$ can be found from the Kirchhoff equation

$$V = U + \int_0^L F(x, t) dx, \tag{5}$$

where V is the voltage applied to the superlattice, while U describes the voltage drop on the contacts (see [17]). If A is the area of the contact, then the density of the current through the superlattice can be expressed via the current density distribution $J(x, t)$ in the superlattice:

$$I(t) = A \int_0^L J(x, t) dx, \tag{6}$$

which can be easily measured in a physical experiment.

2.3. Computation of drift velocity of electrons in an external tilted magnetic field. To find the drift velocity of a particular electron under the effect of electric and magnetic fields, we use the configuration displayed in Fig. 1a. For this configuration, it is assumed that the main axis of the lattice, i.e., the axis such that the layers of semiconductor materials are drawn along it, coincides with the coordinate axis x , vector $B = (B \cos \theta, 0, B \sin \theta)$ of the magnetic field lies in the plane $x - z$, and its angle with the axis x is θ . The electric field $F = (-F, 0, 0)$ is applied along the semiconductor superlattice and its direction is opposite to the direction of the axis x .

Inside any potential well, the potential energy has a minimum providing the localization of the electrons in the first energy minizone and decreasing the probability of the tunnel effect between zones (see [23]). In the semiclassical approach, the motion equation for a particular electron has the following form inside this energy minizone: $\dot{\mathbf{p}}(t) = -e[\mathbf{F} + (\nabla_{\mathbf{p}} E(\mathbf{p}(t)) \times \mathbf{B})]$, where $\mathbf{p}(t) = (p_x(t), p_y(t), p_z(t))$ is the impulse of the electron at time t and $E(\mathbf{p})$ is the dispersion characteristic of the electron in the lower energy minizone provided that the superlattice is tightly bound; i.e., the width of the minizone exceeds 10 meV (see [19]); this dispersion characteristic has the form

$$E = \frac{\Delta}{2} \left[1 - \cos \left(\frac{p_x d}{\hbar} \right) \right] + \frac{p_y^2 + p_z^2}{2m^*}. \tag{7}$$

In relation (7), Δ is the width of the energy minizone, d is the period of the semiconductor superlattice, and m^* is the efficient electron mass. Equation (7) can be represented by the following equations for the impulse components (see [19]):

$$\dot{p}_x(t) = eF - \omega_{\perp} p_y(t), \quad (8)$$

$$\dot{p}_y(t) = \frac{d\Delta m^* \omega_{\perp}}{2\hbar} \sin\left(\frac{p_x(t)d}{\hbar}\right) - \omega_p p_z(t), \quad (9)$$

$$\dot{p}_z(t) = \omega_p p_y(t), \quad (10)$$

where $\omega_p = eB \cos \theta / m^*$ and $\omega_{\perp} = eB \sin \theta / m^*$ are the cyclotron frequencies corresponding to components B_x and B_z of the magnetic field. The velocity of the electron along direction x is determined by the relation

$$v_x(t) = \dot{x}(t) = v_0 \sin\left(\frac{p_x(t)d}{\hbar}\right), \quad (11)$$

its greatest value is $v_0 = \Delta d / (2\hbar)$. To find the drift velocity v_d of a particular electron with an initial impulse $\mathbf{P}_0 = (p_{0x}, p_{0y}, p_{0z})$, the approach proposed by Esaki and Tsu (see [8, 20]) is used:

$$v_d(\mathbf{P}_0) = \frac{1}{\tau} \int_0^{\infty} v_x(t) \exp(-t/\tau) dt, \quad (12)$$

where τ is the scattering time for electrons, including both elastic and inelastic scattering (see [17]).

As noted above, to approximate strong links, it is important to consider the electron transport only in the lower minizone of the superlattice: this simplifies the simulation of processes in semiconductor superlattices in the described model. Additionally, it is assumed that the Landau–Zener tunnel effect between minizones can be disregarded and the equilibrium concentration of the carriers is the same for all superlattice layers provided that there is no field. Note that such approximations are broadly used to simulate the charge transportation in semiconductor structures and they describe experimental results well (see, e.g., [11, 24, 25]).

3. SELF-CONSISTENT NUMERICAL MODELS OF SUPERLATTICES

The numerical model for the investigation of the dynamics of a semiconductor superlattice under the effect of an external magnetic field is created by the mathematical model described in Section 2.

To create the numerical model, we have to reduce all the main equations to a dimensionless form. In such a case, the collective dynamics of the charge carriers in a semiconductor superlattice are described by the following self-consistent system of differential equations, including the dimensionless continuity equation describing the time variation of the electron concentration and the dimensionless Poisson equation describing the distribution of the electric field along the superlattice:

$$\frac{\partial n}{\partial t} = -\beta \frac{\partial J}{\partial x}, \quad (13)$$

$$\frac{\partial F}{\partial x} = v(n - 1), \quad (14)$$

where $\beta = v_0' \tau' / L'$ characterizes the greatest electron velocity in the minizone, while $v = eL'n_D' / (F_c' \epsilon_0 \epsilon_r)$ is proportional to the equilibrium charge concentration. In those equations, variables with dimensions are primed (e.g., n' , x' , and t'), while the dimensionless ones are not (e.g., n , x , and t). To pass to dimensionless variables, we use the relations

$$x = x'/L', \quad t = t'/\tau', \quad n = n'/n_D', \quad J = J' / (en_D' v_0'), \quad F = F' / F_c', \quad F_c = \hbar / (ed'\tau'), \quad (15)$$

where $e > 0$ is the electron charge and F_c' corresponds to the value of the electric field strength such that the period of the Bloch oscillations coincides with the scattering time and is used to normalize the electric field. The parameter $v_0 = \Delta'd' / (2\hbar)$ corresponds to the greatest possible value of the dimensionless drift

velocity. The parameters $\delta = [\tau'_e / (\tau'_e + \tau'_i)]^{1/2}$ and $\tau' = \delta\tau'_i$ characterize the scattering of electrons and depend on the elastic scattering time τ'_e and inelastic scattering time τ'_i .

System (13) and (14) is solved with respect to the dimensionless variables $n(x, t)$ and $F(x, t)$, where $n(x, t)$ is the dimensionless volume density of charge carriers, $F(x, t)$ is the distribution of the electric field, $J(x, t)$ is the density of the current through the superlattice, and x and t are the dimensionless coordinate and time. In the drift approximation for low temperatures T' , the distribution of the current density is computed as follows: $J = n v_d(F)$. To find the dependence of the drift velocity $v_d(F)$ for particular parameters of the external magnetic field, we numerically integrate Eq. (12).

Suppose that the emitter and collector have ohmic contacts and the density of the current $J(0, t)$ through the emitter is determined by the contact conductivity. Then, due to Ohm's law, we have the boundary-value condition $J(0, t) = sF(0, t)$, where $s = \sigma' F'_0 / (en'_D \omega'_{B0} d')$ corresponds to the dimensionless electric conductivity of the emitter, related to the dimensional quantity σ' . The dimensionless value of the voltage drop on the superlattice $U_{SL} = U'_{SL} / (F'_c L')$ can be found from the condition

$$U_{SL} = \int_0^L F dx, \tag{16}$$

where $L = L'/d'$ is the length of the system.

In order to numerically integrate the above system of equations, we decompose the superlattice into a sufficiently large number N of narrow layers with width Δx . In each m th layer, the concentration n_m of electrons is assumed to be constant. Denote the concentration of electrons in the m th layer by n_m . Then the equation describing the evolution of the charge density in the m th layer can be represented (see [26]) as the following discrete analog of the continuous equation (13):

$$\Delta x \frac{dn_m}{dt} = \beta(J_{m-1} - J_m), \quad m = 1, \dots, N, \tag{17}$$

where J_{m-1} and J_m are the densities of the current through the upper and lower boundary of the m th layer, respectively. The current density J_m is defined as $J_m = n_m v_d(F_m)$, where v_d describes the drift electron velocity depending on the value of the electric field F_m in the m th layer. For any m the following discrete representation of the Poisson equation is valid for the m th layer:

$$F_{m+1} = v(n_m - 1) + F_m, \quad m = 1, \dots, N. \tag{18}$$

In this finite-difference model, the voltage drop on the superlattice is defined with the help of relation (16), where the integral is changed for summation over all N layers of the digitized model:

$$U_{SL} = \frac{\Delta x}{2} \sum_{m=1}^N (F_m + F_{m+1}). \tag{19}$$

According to [17], the intensity (in dimensional quantities) of the current through the superlattice can be found as follows:

$$I = \frac{A' en'_D v_0}{N + 1} \sum_{m=0}^N J_m, \tag{20}$$

where A' is the area of the cross section of the semiconductor superlattice.

4. SOFTWARE PACKAGE: DESCRIPTION

The developed software package aimed at simulating nonstationary nonlinear processes in semiconductor superlattices numerically is based on the mathematical model described above and the numerical model developed based on it. Note that the developed software package provides the possibility to analyze physical processes and optimize the characteristics of the generation of devices based on superlattices.

The functional scheme of subroutine interaction is displayed in Fig. 2. The simulation program for superlattice processes includes the *INPUT* subroutine aimed at assigning exact physical parameters of the

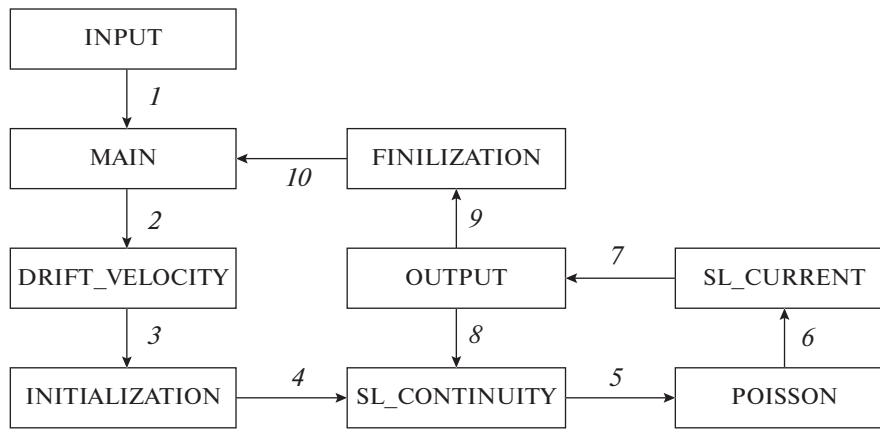


Fig. 2. Functional interaction scheme for subroutines of software package.

investigated nanostructure, including its period, the length and width of the minizone, and the parameters of the external magnetic field (the induction and tilt angle), as well as the main parameters of the numerical scheme. To analyze the behavior of a semiconductor superlattice in a given range of parameter values, we can use this subroutine to assign the time of the transition process, the desired digitization of the recorded time series, and the time range to record the spatial-temporal distributions of the charge concentration, current density, and field density in the layers of the nanostructure. The next step (1) is to invoke the *MAIN* subroutine launching the subroutines computing the charge dynamics in the superlattice according to the model described in Sections 2 and 3. This subroutine changes the control parameter (e.g., the supply voltage or the parameters of the external magnetic field). Completing the computation of the temporal realization (for any value of the control parameter), the *MAIN* subroutine records the oscillation power and the mean value of the current generated by the superlattice in a file: this is enough to reconstruct the current–voltage characteristic of the simulated sample.

It takes significant resources to solve the above numerical model. Therefore, it is efficient to use dependence of the drift velocity on the electric field strength, found during the computation of the current intensity in any layer of the superlattice. To do this, the *DRIFT_VELOCITY* subroutine (2) is invoked: it computes the drift electron velocity in a wide range of values of the electric field strength provided that the parameters of the external magnetic field are given. In the sequel, the drift electron velocity is found by means interpolating the tabulated dependence. In the next step (3), the *SL_INIT* subroutine presets all variables, defines the initial charge and field distribution in nanostructure layers, and open files to record the realizations.

The numerical simulation used to compute the spatial-temporal charge dynamics in the superlattice layers is implemented in the *SL_CONTINUITY* subroutine and *POISSON* subroutine: they compute the change of the concentration of electrons (4) and of the field strength (5) in any layer of the nanostructure, taking into account the previous state and the applied feed voltage. The resulting current generated by the superlattice is computed by the *SL_CURRENT* subroutine (6). Then the *SL_OUTPUT* subroutine (7) records the found valued of the current, as well as the spatial-temporal distributions of the charge concentration in the superlattice levels in a file. Then either the next iteration (8) is launched or the control is forwarded to the *FINALIZATION* subroutine (9) cleaning all arrays containing information about the previous state of the system and closing the recorded files. Then the *MAIN* subroutine either changes the value of the control parameter and launches the computation of a new realization or completes the work of the program.

5. DYNAMICS OF SEMICONDUCTOR SUPERLATTICES: SIMULATION RESULTS

We briefly provide several important simulation results for processes in semiconductor superlattices. The real semiconductor superlattice investigated in [11, 24, 25] is taken as a base model to estimate the physical parameters. The following dimensional parameters of the main physical values describing the system correspond to that nanostructure: $d' = 8.3$ bicrons is the superlattice period, $L' = 115.2$ bicrons is its length, $A' = 5 \times 10^{-10}$ is the cross-section area, $\Delta' = 19.1$ mev is the minizone width, $n'_D = 3 \times 10^{22} \text{ m}^{-3}$ is the equilibrium concentration of the electrons determined by the alloying level, $m^* = 0.067m_e$, where

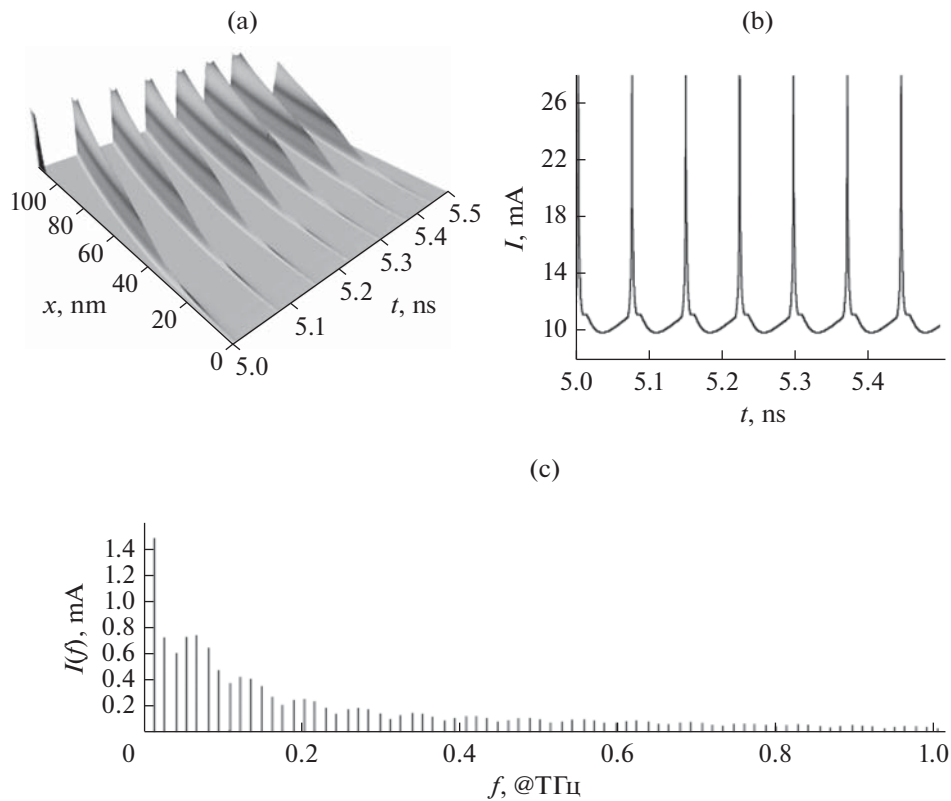


Fig. 3. Spatial-temporal charge dynamics in layers of superlattice (a), temporal current realization (b), and their oscillation spectrum (c) assuming that feed voltage of superlattice is 610 mV and $B = 0$ T.

m_e is the mass of a free electron, $F_c' = 3.1725 \times 10^5$ V/m is the value of the electric field, corresponding to the greatest dependence of the drift velocity, and ϵ_0 and $\epsilon_r = 12.5$ are the electric constant and the relative dielectric constant of the material, respectively.

For this paper, the following parameters of the finite-difference scheme are selected: $N = 480$ and $\Delta t = 5 \times 10^{-4}$. For these values, the numerical scheme is stable and provides the necessary computation precision.

5.1. Semiconductor superlattices: spatial-temporal charge dynamics and current oscillation spectral distributions. To understand processes in semiconductor nanostructures, the temporal dynamics of electron domains in its layers presents the primary interest. Figure 3a displays a typical spatial-temporal distribution for the charge concentration in a superlattice in the generation mode ($V = 610$ mV) for the absence of a magnetic field. The charge domain arises near the emitter ($x = 0$) of the nanostructure and the domain concentration of electrons is low. The charge domain concentration sharply increases (from 10 to 50 bicrons) during the movement along the superlattice. Then the velocity goes down (60 bicrons) and slightly increases afterwards (from 60 to 115 bicrons). The domain output is followed by a sharp jump of the current value on the temporal realization (see Fig. 3b), which causes the presence of clear higher harmonics in the spectrum of oscillations (see Fig. 3c) such that their power is comparable with the power of the fundamental generation frequency ($f_0 = 13.7$ GHz) achieving values from 200 to 300 GHz. Thus, a semiconductor can be used to generate the electromagnetic emission from the sub-terahertz and terahertz ranges.

5.2. Absorption and impedance of semiconductor superlattices. From a practical viewpoint, it is important to investigate the high-frequency superlattice impedance because this allows us to analyze the superlattice behavior in various electronic schemes and devices including a superlattice generating or amplifying high-frequency signals. It is also important to investigate the absorption value to estimate the absorption of the electromagnetic power and to find domains where the external signals are amplified by the nanostructure.

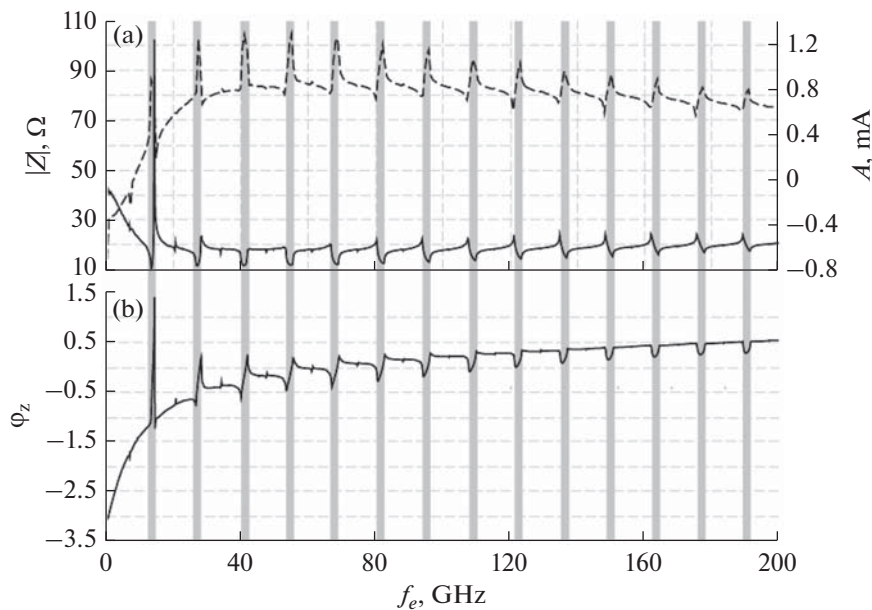


Fig. 4. Dependence of (a) absorption (dotted curve) and amplitude (dense curve) and (b) phase of high-frequency impedance on frequency of external action. Constant voltage 610 mV applied to superlattice, amplitude V_m of external signal is 60 mV, and $B = 0$ T. Synchronization regions are marked in gray.

In our case, we consider the dynamics of a semiconductor superlattice such that there are no external magnetic fields; however, an external periodic signal is applied to the superlattice. To simulate the external periodic signal affecting the nanostructure, the external alternating voltage $V_{\text{ext}}(t) = V_m \cos(2\pi f_e t)$, where V_m and f_e are the amplitude and frequency of the external signal, respectively, is added to the constant voltage applied to the superlattice. The approach developed in [27] is used to compute the high-frequency impedance. The absorption of the external signal is computed according to [28].

It is found that synchronization with the external periodic signal leads to a substantial increase of its absorption A (see Fig. 4a), while the behavior of the impedance amplitude Z is the opposite. Also, a strong jump of the impedance amplitude takes place on the boundary of the first synchronization hook and weaker jumps take place in other synchronization regions. Note that the absorption takes negative values for low frequencies (below 9 GHz), which means that the superlattice can be used as an amplifier of the electromagnetic emission (in this frequency range). In [27], it is shown that the impedance phase φ_z (see Fig. 4b) varies (within the synchronization region) between 0 and π/n , where n is the number of the synchronization hook. In the asynchronous mode, the phase between synchronization hooks is approximately constant. The found effects can be used to diagnose synchronous modes, while the superlattice is working in the terahertz range and it is hard to execute direct measurements. In particular, it is possible to check whether a synchronous mode is established, detecting a sharp change of the impedance amplitude (this is easily measured in experiments using circuit analyzers) or an increase of the absorption value of the external electromagnetic emission.

5.3. Semiconductor superlattices: dynamics under the action of external magnetic fields. Simulating the influence of external magnetic fields on the superlattice charge dynamics, it is interesting (from the practical viewpoint) to investigate the dependence of power generation on the tilt of the external magnetic field. Figure 5 displays the two-parametric dependence of the current oscillation power generated by the nanostructure on the feed voltage and tilt of the external magnetic field. It is easy to see that the oscillation power depends significantly on the magnetic field tilt. Moreover, there exists an optimum angle θ between 60° and 75° resulting in the power more than tripling compared to the autonomous case (the absence of an external magnetic field is equivalent to the case where $\theta = 0^\circ$). At the same time, the power generation decreases if the applied voltage increases. Note that, in the autonomous case, the oscillation power of the superlattice current increases if the feed voltage increases, which means that the dynamics of the electron domains are substantially modified once an external magnetic field is applied.

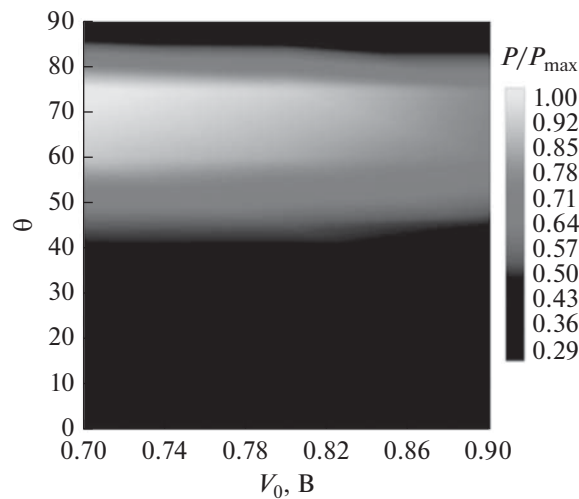


Fig. 5. Two-parametric dependence of current oscillation power on superlattice on tilt of external magnetic field and constant voltage applied to superlattice. Induction B of magnetic field is 7 T.

6. CONCLUSIONS

A software package able to simulate nonstationary processes numerically and optimize the generation characteristics of semiconductor superlattices under the effect of electric and magnetic fields is designed. A number of numerical experiments are executed. The results of these experiments show that the designed package is an efficient tool for studying processes in semiconductor nanostructures and designing devices based on such nanostructures.

ACKNOWLEDGMENTS

This work was supported by the Ministry of Education and Science of the Russian Federation (no. 931 and 3.23.2014/K). This work was supported by the Russian Foundation for Basic Research, project nos. 15-02-00624 and 15-32-20299. This work was supported by grant MK-5426.2015.2 of the President of the Russian Federation for young Russian candidates of sciences.

REFERENCES

1. V. L. Bratman, A. G. Litvak, and E. V. Suvorov, "Mastering the terahertz domain: sources and applications," *Phys. Usp.* **54**, 837–844 (2011).
2. M. Tonouchi, "Cutting-edge THz-technology," *Nat. Photon.*, No. 1, 97–105 (2007).
3. C. R. Sirtori, "Applied physics: bridge for the terahertz gap," *Nature* **417**, 132–133 (2002).
4. Y. Watanabe, K. Kawase, T. Ikari, H. Ito, Y. Ishikawa, and H. Minamide, "Component spatial pattern analysis of chemicals using terahertz spectroscopic imaging," *Appl. Phys. Lett.* **83**, 800–802 (2003).
5. P. H. Siegel, "THz technology," *IEEE Trans. Microwave Theory Tech.* **50**, 910–928 (2002).
6. Ho-Jin Song and T. Nagatsuma, "Present and future of terahertz communications," *IEEE Trans. Terahertz Sci. Technol.* **1**, 256–263 (2011).
7. M. I. Ovsianikov, Yu. A. Romanov, V. N. Shabanov, and R. G. Loginova, "Semiconductor periodic structures," *Sov. Phys. Semicond.* **12**, 1919 (1970).
8. L. Esaki and R. Tsu, "Superlattices and negative differential conductivity in semiconductors," *IBM J. Res. Develop.* **14**, 61–65 (1970).
9. A. Y. Shik, "Superlattices – periodic semiconductor structures," *Sov. Phys. Semicond.* **17**, 1195 (1975).
10. A. O. Selskii, A. A. Koronovskii, A. E. Hramov, et al., "Effect of temperature on resonant electron transport through stochastic conduction channels in superlattices," *Phys. Rev. B* **84**, 235311 (2011).
11. V. A. Maksimenko, V. V. Makarov, A. A. Koronovskii, et al., "The effect of collector doping on the high-frequency generation in strongly coupled semiconductor superlattice," *Europhys. Lett.* **109**, 47007 (2015).
12. V. V. Makarov, A. E. Hramov, A. A. Koronovskii, et al., "Sub-terahertz amplification in a semiconductor superlattice with moving charge domains," *Appl. Phys. Lett.* **106**, 043503 (2015).

13. A. E. Hramov, V. V. Makarov, A. A. Koronovskii, et al., “Subterahertz chaos generation by coupling a superlattice to a linear resonator,” *Phys. Rev. Lett.* **112**, 116603 (2014).
14. G. Belle, J. C. Maan, and G. Weimann, “Measurement of the miniband width in a superlattice with interband absorption in a magnetic field parallel to the layers,” *Solid State Commun.* **56**, 65–68 (1985).
15. A. O. Sel’skii, A. A. Koronovskii, O. I. Moskalenko, A. E. Hramov, T. M. Fromhold, M. T. Greenaway, and A. G. Balanov, “Studying transitions between different regimes of current oscillations generated in a semiconductor superlattice in the presence of a tilted magnetic field at various temperatures,” *Tech. Phys. Lett.* **41**, 768–770 (2015).
16. V. V. Makarov, V. A. Maksimenko, A. O. Selskii, et al., “THz-generation in semiconductor superlattice in the external tilted magnetic field,” *Proc. SPIE* **9322**, 932211 (2015).
17. A. Wacker, “Semiconductor superlattices: a model system for nonlinear transport,” *Phys. Rep.* **357**, 1–111 (2002).
18. L. L. Bonilla and H. T. Grahn, “Nonlinear dynamics of semiconductor superlattices,” *Rep. Prog. Phys.* **68**, 577–683 (2005).
19. T. M. Fromhold, A. Patane, S. Bujkiewicz, et al., “Chaotic electron diffusion through stochastic webs enhances current flow in superlattices,” *Nature* **428**, 726–730 (2004).
20. M. T. Greenaway, A. G. Balanov, E. Scholl, and T. M. Fromhold, “Controlling and enhancing terahertz collective electron dynamics in superlattices by chaos-assisted miniband transport,” *Phys. Rev. B* **80**, 205318 (2009).
21. T. Hyart, J. Mattas, and K. N. Alekseev, “Model of the influence of an external magnetic field on the gain of terahertz radiation from semiconductor superlattices,” *Phys. Rev. Lett.* **103**, 117401 (2010).
22. Yu. A. Romarov, “Nonlinear effects in periodic semiconductor structures,” *Opt. Spectrosc.* **33**, 917–920 (1972).
23. A. Patane, D. Sherwood, L. Eaves, et al., “Tailoring the electronic properties of GaAs/AlAs superlattices by InAs layer insertions,” *Appl. Phys. Lett.* **81**, 661–663 (2002).
24. N. Alexeeva, M. T. Greenaway, A. G. Balanov, et al., “Controlling high-frequency collective electron dynamics via single-particle complexity,” *Phys. Rev. Lett.* **109**, 024102 (2012).
25. D. Fowler, D. P. A. Hardwick, A. Patane et al., “Magnetic-field-induced miniband conduction in semiconductor superlattices,” *Phys. Rev. B* **76**, 245303 (2007).
26. D. Potter, *Computational Physics* (Wiley, London, 1973).
27. A. Jappsen, A. Amann, A. Wacker, E. Scholl, and E. Schomburg, “High-frequency impedance of driven superlattices,” *J. Appl. Phys.* **92**, 3137 (2002).
28. T. Hyart, K. Alekseev, and E. Thuneberg, “Bloch gain in dc-ac-driven semiconductor superlattices in the absence of electric domains,” *Phys. Rev. B* **77**, 165330 (2008).

Translated by A. Muravnik

SPELL: 1. OK